



1

1 **Autoxidation of terpenes, a common pathway in tropospheric**
2 **and low temperature combustion conditions: the case of**
3 **limonene and α -pinene.**

4 Roland Benoit¹ Nesrine Belhadj^{1,2}, Maxence Lailliau^{1,2}, and Philippe Dagaut¹

5 ¹CNRS-INSIS, ICARE, Orléans, France, roland.benoit@cnrs-orleans.fr, nesrine.belhadj@cnrs-orleans.fr,
6 maxence.lailliau@cnrs-orleans.fr, dagaut@cnrs-orleans.fr

7 ²Université d'Orléans, Orléans, France

8 **Correspondence:** Roland Benoit (roland.benoit@cnrs-orleans.fr)

9

10 **Abstract.**

11 The oxidation of monoterpenes under atmospheric conditions has been the subject of numerous studies. They were
12 motivated by the formation of oxidized organic molecules (OOM) which, due to their low vapor pressure,
13 contribute to the formation of secondary organic aerosols (SOA). Among the different reaction mechanisms
14 proposed for the formation of these oxidized chemical compounds, it appears that the autoxidation mechanism,
15 involving successive events of H-migration and O₂ addition, common to both low-temperature combustion and
16 atmospheric conditions, is leading to the formation of highly oxidized molecules (HOM). In atmospheric
17 chemistry, the importance of autoxidation compared to other oxidation pathways has been the topic of numerous
18 studies. Conversely, in combustion, autoxidation under cool flame conditions is the main oxidation process
19 commonly taken into account. An analysis of oxidation products detected in both conditions was performed, using
20 the present combustion data and literature data from tropospheric oxidation studies, to investigate possible
21 similarities in terms of observed chemical formulae of products. To carry out this study, we chose two terpenes,
22 α -pinene and limonene (C₁₀H₁₆), among the most abundant biogenic components in the atmosphere, and
23 considered in many previous studies. Also, these two isomers were selected for the diversity of their reaction sites
24 (exo- and endo- carbon-carbon double bonds). We built an experimental database consisting of literature
25 atmospheric oxidation data and presently obtained combustion data for the oxidation of the two selected terpenes.
26 In order to probe the effects of the type of ionization used in mass spectrometry analyses on the detection of
27 oxidation products, we used heated electrospray ionization (HESI) and atmospheric pressure chemical ionization
28 (APCI), in positive and negative modes. The oxidation of limonene-oxygen-nitrogen and α -pinene-oxygen-
29 nitrogen mixtures was performed using a jet-stirred reactor at elevated temperature (590 K), a residence time of 2
30 s, and atmospheric pressure. Samples of the reacting mixtures were collected in acetonitrile and analyzed by high-
31 resolution mass spectrometry (Orbitrap Q-Exactive) after direct injection and soft ionization, i.e. (+/-) HESI and
32 (+/-) APCI. This work shows a surprisingly similar set of chemical formulae of products, including oligomers,
33 formed in cool flames and under simulated atmospheric conditions. Data analysis showed that a non-negligible
34 subset of chemical formulae is common to all experiments independently of experimental parameters. Finally, this
35 study indicates that more than 40% of the detected chemical formulae in this full dataset can be ascribed to an
36 autoxidation mechanism.

37



2

38 1 Introduction

39 The links between atmospheric and combustion chemistry have often been studied from the point of view of
40 tropospheric reactions of combustion effluents or pollutants, e.g., oxidation of volatile organic compounds,
41 nitrogen oxides reactions, sulfur chemistry (Barsanti et al., 2017; Shrivastava et al., 2017; Zhao et al., 2018; Bianchi
42 et al., 2019). Climate change and the increase of large wildfire events have profoundly modified the relationship
43 between atmospheric chemistry and combustion at large. When studying the oxidation of chemicals and the
44 formation of SOA in the atmosphere, it becomes necessary to determine the contribution of different oxidation
45 pathways pertaining to atmospheric chemistry, combustion chemistry, or both.

46 In low-temperature combustion (cool flame) the formation of oxidized organic molecules (OOM) is mainly
47 attributed to autoxidation reactions (Belhadj et al., 2021; Benoit et al., 2021), whereas in atmospheric chemistry, it
48 is only relatively recently that this pathway has been considered (Vereecken et al., 2007; Crouse et al.,
49 2013; Jokinen et al., 2014a; Berndt et al., 2015; Jokinen et al., 2015a; Berndt et al., 2016; Iyer et al., 2021). Also, it
50 has been identified that highly oxygenated molecules (HOMs), a source of secondary organic aerosols (SOA), can
51 result from autoxidation processes (Wang et al., 2021; Tomaz et al., 2021; Bianchi et al., 2019). Modeling studies
52 complemented by laboratory experiments showed that autoxidation mechanisms proceed simultaneously on
53 different RO_2^\cdot radicals and leads to, through isomerization and addition of O_2 , the production of a wide range of
54 oxidized compounds in a few hundredths of a second (Jokinen et al., 2014a; Berndt et al., 2016; Bianchi et al.,
55 2019). Autoxidation is based on an H-shift and oxygen addition which starts with the initial production of RO_2^\cdot
56 radicals. This mechanism can repeat itself several times and lead to recurrent oxygen additions to form HOMs: $\text{R} +$
57 $\text{O}_2 \rightleftharpoons \text{ROO}^\cdot$ (first O_2 -addition); $\text{ROO}^\cdot \rightleftharpoons \text{QOOH}$ (H-shift); $\text{QOOH} + \text{O}_2 \rightleftharpoons \text{OOQOOH}$ (second O_2 -addition);
58 $\text{OOQOOH} \rightleftharpoons \text{HOOQOOH}$ (H-shift); $\text{HOOQOOH} + \text{O}_2 \rightleftharpoons (\text{HOO})_2\text{QOO}^\cdot$ (third O_2 -addition); $(\text{HOO})_2\text{QOO}^\cdot$
59 $\rightleftharpoons (\text{HOO})_2\text{QOOH}$ (H-shift); $(\text{HOO})_2\text{QOOH} + \text{O}_2 \rightleftharpoons (\text{HOO})_3\text{QOO}^\cdot$ (fourth O_2 -addition) etc. Recent works
60 have shown that, under certain atmospheric conditions, this autoxidation mechanism could be competitive with
61 other reaction pathways involving RO_2^\cdot radicals (Bianchi et al., 2019), e.g., the carbonyl channel ($\text{ROO}^\cdot \rightarrow \text{R}_\text{H}\text{O}$
62 $+ \text{OH}$), the hydroperoxide channel ($\text{ROO}^\cdot + \text{HOO}^\cdot \rightarrow \text{ROOH} + \text{O}_2$ and $\text{RO}^\cdot + \text{OH} + \text{O}_2$), disproportionation
63 reactions ($\text{ROO}^\cdot + \text{R}'\text{OO}^\cdot \rightarrow \text{RO}^\cdot + \text{R}'\text{O}^\cdot + \text{O}_2$ and $\text{R}_\text{H}\text{O} + \text{R}'\text{OH} + \text{O}_2$), accretion reactions ($\text{ROO}^\cdot + \text{R}'\text{OO}^\cdot \rightarrow$
64 $\text{ROOR}' + \text{O}_2$). A study published in 2021 showed that the oxidation of alkanes follows this autoxidation
65 mechanism under both atmospheric and combustion conditions (Wang et al., 2021). Also, that work confirmed
66 that internal H-shifts in autoxidation can be promoted by the presence of functional groups, as predicted earlier
67 (Otkjær et al., 2018) for RO_2^\cdot radicals containing OOH, OH, OCH_3 , CH_3 , $\text{C}=\text{O}$, or $\text{C}=\text{C}$ groups. To further assess
68 the importance of these pathways, available data must be compared along with their experimental specificities. In
69 laboratory studies under simulated atmospheric conditions, oxidation occurs at near-ambient temperatures (250-
70 300 K), at atmospheric pressure, in the presence of ozone and/or OH^\cdot radicals, and with low initial terpene
71 concentrations. In combustion, the OH^\cdot radical, temperature, and pressure are driving autoxidation. Initial reactant
72 concentrations are generally higher compared to atmospheric conditions, so as to compensate for the absence of
73 ozone and get oxidation to proceed, since terpenes, as other hydrocarbons, react very slowly with O_2 . Rising
74 temperature increases isomerization rates and favors autoxidation, at the expense of other possible reactions of
75 RO_2^\cdot radicals. In atmospheric chemistry, at near room temperature, autoxidation can be initiated via two reaction
76 mechanisms: reactions with ozone or with the OH^\cdot radical. Suppression of one of these pathways by scavengers



3

77 generally changes the amount of products formed (sometimes a drastic decrease >90% was observed (Kenseth et
78 al., 2018;Meusinger et al., 2017;Pospisilova et al., 2020)), but does not affect the diversity of observed chemical
79 formulae (Zhao et al., 2018;Pospisilova et al., 2020). It has been reported earlier that a temperature rise from 250
80 to 273K does not affect the distribution of HOMs (Quéléver et al., 2019) whereas Trostl et al. suggested that the
81 distribution of HOMs is affected by temperature, α -pinene or particle concentration (Tröstl et al., 2016). Similarly,
82 the experiments of Huang et al. performed at different temperatures (223 K and 296 K) and precursor concentration
83 (α -pinene 0.714 and 2.2 ppm) suggested that the physicochemical properties, such as the composition of the
84 oligomers, can be affected by a variation of temperature (Huang et al., 2018). Both in combustion and atmospheric
85 chemistry, autoxidation can yield highly oxygenated molecules (HOMs), e.g., compounds containing more than 7
86 oxygen atoms (Benoit et al., 2021;Bianchi et al., 2019). The term ‘HOM’ is generally associated with atmospheric
87 chemistry (Bianchi et al., 2019), but this nomenclature does not specify the chemical properties of a compound.
88 In other words, in combustion we can also observe highly oxidized chemical compounds similar to those relevant
89 to atmospheric chemistry. The broad range of chemical molecules formed and the impact of the experimental
90 conditions on their character remain a subject for atmospheric chemistry as well as combustion chemistry studies.
91 Moreover, whatever the mechanism of aerosol formation, i.e., oligomerization, addition, or accretion, their
92 composition will be linked to that of the initial radical pool (Tomaz et al., 2021).

93 In low-temperature combustion, when the temperature is increased, autoxidation rate goes through a maximum
94 between 500 and 670 K, depending on the nature of the fuel (Belhadj et al., 2020;Belhadj et al., 2021), and the rate
95 of formation of HOM also increases (Bianchi et al., 2019). Therefore, temperature has a measurable effect on the
96 amount of HOMs formed (Wang et al., 2021). In low-temperature combustion chemistry as in atmospheric
97 chemistry, the oxidation of a chemical compound leads to the formation of several thousands of chemical products
98 which result from successive additions of oxygen, isomerization, accretion, fragmentation, and oligomerization
99 (Benoit et al., 2021). The exhaustive analysis of chemical species remains, in the current state of instrumental
100 limitations, impossible. This would consist in analyzing several thousands of molecules in MS² mode using
101 separative techniques such as ultra-high pressure liquid chromatography (UHPLC) or ion mobility spectrometry
102 (IMS) (Krechmer et al., 2016;Kristensen et al., 2016). Nevertheless, it is possible to classify these molecular
103 species, considering only C_xH_yO_z compounds, according to various criteria accessible via graphic tools
104 representation such as van Krevelen diagrams, double bond equivalent number (DBE), and average carbon
105 oxidation state (OSc) versus the number of carbon atoms (Kourtchev et al., 2015;Nozière et al., 2015). Such
106 postprocessing of large datasets has the advantage of immediately highlighting families of compounds or
107 physicochemical properties such as the condensation of molecules (vapor pressure), the large variety of oxygenated
108 products (C_xH_yO₁₋₁₅ in the present experiments) and the formation of oligomers (Kroll et al., 2011;Xie et al., 2020).

109 In addition to the recent studies focusing on the first steps of autoxidation, a more global approach, based on the
110 comparison of possible chemical transformations related to autoxidation in low temperature combustion and
111 atmospheric chemistry, is needed for evaluating the importance of autoxidation under tropospheric and low-
112 temperature combustion conditions. In order to study the effects of ozonolysis and combustion on the diversity of
113 chemical molecules formed by autoxidation, we have selected α -pinene and limonene, two terpene isomers among
114 the most abundant in the troposphere. Limonene has a single ring structure and two double bonds, one of which is
115 exocyclic. α -Pinene has a bicyclic structure and a single endo-cyclic double bond. These two isomers with their
116 distinctive characters are good candidates for studying autoxidation versus initial chemical structure and



4

117 temperature. For α -pinene, in addition to the reactivity of its endo-cyclic double bond, products of ring opening of
118 the cyclobutyl group have been detected, which could explain the diversity of observed oxidation products (Kurtén
119 et al., 2015; Iyer et al., 2021). This large pool of products is increased in the case of limonene by the presence of
120 two double bonds (Hammes et al., 2019; Jokinen et al., 2015a). Nevertheless, the diversity of oxidation products
121 can be compensated by similarities in terms of reaction mechanisms and intermediates formed through
122 autoxidation (Savee et al., 2015).

123 In the present work, which is a prolongation of that published earlier for the oxidation of limonene alone (Benoit
124 et al., 2021), we oxidized α -pinene and limonene in a jet-stirred reactor at atmospheric pressure, excess of oxygen,
125 and elevated temperature. Then, we characterized the impact of using different ionization techniques (HESI and
126 APCI) in positive and negative modes on the pool of detected chemical formulae. The particularities of each
127 ionization mode were analyzed to identify the most suitable ionization technique for exploring the formation of
128 autoxidation products under low temperature combustion. Chemical formulae detected here and in atmospheric
129 chemistry studies were compiled and tentatively used to evaluate the importance of autoxidation under both
130 conditions.

131 2 Experiments

132 2.1 Oxidation experiments

133 The present experiments were carried out in a fused silica jet-stirred reactor (JSR) setup presented earlier (Dagaut
134 et al., 1986; Dagaut et al., 1988) and used in previous studies (Dagaut et al., 1987; Benoit et al., 2021; Belhadj et al.,
135 2021). The two isomers α -pinene and limonene were studied separately. As in earlier works (Benoit et al.,
136 2021; Belhadj et al., 2021), α -pinene (+), 98% pure from Aldrich and limonene (R)-(+), >97% pure from Sigma,
137 were pumped by an HPLC pump (Shimadzu LC10 AD VP) with an online degasser (Shimadzu DGU-20 A3) and
138 sent to a vaporizer assembly where it was diluted by a nitrogen flow. Each terpene isomer and oxygen, both diluted
139 by N_2 , were sent separately to a 42 mL JSR to avoid oxidation before reaching 4 injectors (nozzles of 1 mm I.D.)
140 providing stirring. The flow rates of nitrogen and oxygen were controlled by mass flow meters. Good thermal
141 homogeneity along the vertical axis of the JSR was recorded (gradients of < 1 K/cm) by thermocouple
142 measurements (0.1 mm Pt-Pt/Rh-10% wires located inside a thin-wall silica tube). In order to observe the oxidation
143 of these isomers, which are not prone to strong self-ignition, the oxidation of 1% of these chemical compounds
144 ($C_{10}H_{16}$) under lean fuel conditions (equivalence ratio 0.25, 56% O_2 , 43% N_2), experiments were carried out at 590
145 K, atmospheric pressure, and a residence time of 2 s. Under these conditions, the oxidation of the two isomers is
146 initiated by slow H-atom abstraction by molecular oxygen. The fuel radicals react rapidly with O_2 to form peroxy
147 radicals which undergo further oxidation, characteristic of autoxidation. The absence of ozone, and no need for
148 the addition of a scavenger, allow probing reaction mechanisms and observing chemical species potentially
149 specific to autoxidation initiated by OH radicals. A 2 mm I.D. probe was used to collect samples. To measure low-
150 temperature oxidation products ranging from early oxidation steps to highly oxidized molecules, the sonic probe
151 samples were bubbled in cooled acetonitrile (UHPLC grade ≥ 99.9 , $T = 0^\circ C$, 250 mL) for 90 min. The resulting
152 solution was stored in a freezer at $-15^\circ C$.

153



5

154 2.2 Chemical analyses

155 Analyses of samples collected in acetonitrile were performed by direct sample instillation (rate: 3 μL/min and
156 recorded for 1 min for data averaging) in the ionization chamber of a high-resolution mass spectrometer (Thermo
157 Scientific Orbitrap® Q-Exactive, mass resolution 140,000 and mass accuracy <0.5 ppm RMS). Both heated
158 electrospray ionization (HESI) and atmospheric chemical ionization (APCI) were used in positive and negative
159 modes for the ionization of products. HESI settings were: spray voltage 3.8 kV, T vaporizer of 150°C, T capillary
160 200°C, sheath gas flow of 8 arbitrary units (a.u.), auxiliary gas flow of 1 a.u., sweep gas flow of 0 a.u.. In APCI,
161 settings were: spray voltage 3.8 kV, vaporizer temperature of 150°C, capillary temperature of 200°C, sheath gas
162 flow of 8 a.u., auxiliary gas flow of 1 a.u., sweep gas flow of 0 a.u., corona current of 3 μA. In order to avoid
163 transmission and detection effects of ions depending on their mass inside the C-Trap (Hecht et al., 2019),
164 acquisitions with three mass ranges were performed (m/z 50-750; m/z 150-750; m/z 300-750). The upper limit of
165 m/z 750 was chosen because of the absence of signal beyond this value. We verified that no significant oxidation
166 occurred in the HESI and APCI ion sources by injecting a limonene-ACN mixture. The optimization of the
167 Orbitrap ionization parameters in HESI and APCI did not show any clustering phenomenon for these two isomers.
168 The parameters evaluated were: injection source - capillary distance, vaporization and capillary temperatures,
169 applied difference of potential, injected volume, flow rate of nitrogen in the ionization source. Positive and
170 negative HESI mass calibrations were performed using Pierce™ calibration mixtures (Thermo Scientific).
171 Chemical compounds with relative intensity less than 1 ppm to the highest mass peak in the mass spectrum were
172 not considered. Nevertheless, it should be considered that some of the molecules presented in this study could
173 result from our experimental conditions (continuous flow reactor, reagent concentration, temperature, reaction
174 time) and to some extent from our acquisition conditions, different from those of the previous studies (Deng et al.,
175 2021; Quéléver et al., 2019; Meusinger et al., 2017; Krechmer et al., 2016; Tomaz et al., 2021; Fang et al.,
176 2017; Witkowski and Gierczak, 2017; Jokinen et al., 2015b; Nørgaard et al., 2013; Bateman et al., 2009; Walser et
177 al., 2008; Warscheid and Hoffmann, 2001; Hammes et al., 2019; Kundu et al., 2012). Indeed, the use of a continuous
178 flow reactor operating at elevated temperature, as well as a high initial concentration of reagents can induce the
179 formation of combustion-specific products, which does not exclude their possible formation under atmospheric
180 conditions.

181 3 Data Processing

182 High resolution mass spectrometry (HR-MS) generates a large amount of data that is difficult to fully analyze by
183 sequential methods. When the study requires the processing of several thousands of molecules, the use of statistical
184 tools and graphical representation means becomes necessary. In this study, we have chosen to use the van Krevelen
185 diagram (Van Krevelen, 1950) by adding an additional dimension, the double bond equivalent (DBE). The DBE
186 number represents the sum of unsaturation and rings present in a chemical compound (Melendez-Perez et al.,
187 2016).

$$188 \quad \text{DBE} = 1 + C - \text{H}/2 - \text{O}$$

189 This number is independent of the number of oxygen atoms, but changes with the number of hydrogen atoms.
190 Decimal values of this number, which correspond to an odd number of hydrogen atoms, were not considered in
191 this study. Then, duplications of chemical formulae in the O/C vs. H/C space are eliminated. The oxidation state



6

192 of carbon (OSc) provides a measure of the degree of oxidation of chemical compounds (alcohols, aldehydes,
193 carboxylic acids, esters, ethers and ketones, but not peroxides) (Kroll et al., 2011). This provides a framework for
194 describing the chemistry of organic species. It is defined by the following equation:

$$195 \quad \text{OSc} \approx 2 \text{O/C} - \text{H/C}$$

196 **4 Results and discussion**

197 The oxidation of the two isomers, α -pinene and limonene ($\text{C}_{10}\text{H}_{16}$), was studied at 590 K, under atmospheric
198 pressure, with a residence time of 2 s and a fuel concentration of 1%. Under these conditions, the formation of
199 peroxides by autoxidation at low temperature should be optimal (Belhadj et al., 2021), even if the conversion of
200 the fuels remains moderate.

201 **4.1 Characterization of ionization sources**

202 First, we have studied the impact of APCI and HESI sources, in positive and negative modes, on the chemical
203 formulae detected. The HESI and APCI sources in positive and negative mode were used and their operating
204 parameters were varied, i.e., temperature, gas flow and accelerating voltage (see Section 2). For each polarity, only
205 ions composed of carbon, hydrogen (even numbers) and oxygen were considered. Molecular duplicates inherent
206 to mass range overlaps were excluded. Chemical formulae with relative intensity less than 1 ppm with respect to
207 the highest mass peak of the mass spectrum were not considered. By following these rules, we obtained a different
208 number of ions depending on the ionization source and the polarity used. Table 1 shows the number of ions
209 according to the experimental conditions and the discrimination rules.

210 **Table 1.** Number of ions detected for each source in positive and negative modes.

Ionization source	α -Pinene		Limonene	
APCI	646 (+)	503(-)	1321(+)	1346(-)
HESI	594(+)	693(-)	1017(+)	1864(-)

211

212 Each combination of ionization sources and polarity generated a set of chemical formulae. To make a meaningful
213 comparison between the positive and negative ions data, the chemical formulae used were the precursors of the
214 ions identified in the mass spectra. These sets have common data, but also specific chemical formulae. For a given
215 ionization source, less than 50% of the chemical formulae are common to both polarities. In other words, between
216 30 and 50% of molecular species are ignored when using a single polarity. It is therefore essential to use both
217 polarities in order to better describe all the species present. The HESI source data were compared to the APCI data
218 (Tables 2 and 3), showing an increase of the number of chemical formulae detected by 20 to 30%. This increase
219 is characterized by a better detection of negatively ionized species and those with a higher unsaturation number
220 (DBE). In order to evaluate further the interest for using these ionization sources, we compiled these data in Venn
221 diagrams and proposed a visualization of these sets with a van Krevelen representation; we added the number of
222 DBE in the third dimension. These results are presented in Tables 2 and 3.



7

223 In positive ionization mode, independently of the ionization source and in addition to the common molecular
224 formulae, we detected products with an O/C ratio < 0.2 whereas in the negative ionization mode, we detected
225 molecular formulae with an O/C ratio > 0.5 . In addition to these observations, we noted that HESI is more
226 appropriate for studying products with a large number of unsaturation ($DBE > 5$). Finally, for an optimal detection
227 of the oxidation products, it is necessary to consider the transmission limits of the C-Trap. Here, we could increase
228 by more than 60% the number of molecular formulae detected using several mass ranges for data acquisition. The
229 most appropriate ionization polarity to be used is tight to chemical functions present in products to be detected.
230 We could increase by 30 to 100% the number of chemical formulae detected by using both positive and negative
231 ionization modes. The ionization source used is also important. We could increase the number of detected chemical
232 formulae by 20 to 30% using HESI. We believe that this approach to data validation and these results, although
233 specific to this study, are applicable to any characterization by Orbitrap.

234



8

235 **Table 2.** Representation of the mass spectrometry data characterizing the oxidation of α -pinene and
 236 limonene (ionization source: APCI positive and negative mode, JSR experiments).

	α -Pinene			Limonene		
Source and mode	APCI ⁺		APCI ⁻	APCI ⁺		APCI ⁻
Number of compounds	646		503	1321		1346
Distribution	specific to positive mode 327	common 319	specific to negative mode 174	specific to positive mode 516	common 805	specific to negative mode 542
Venn graph	<p>Total : 820</p>			<p>Total : 1863</p>		
VK vs DBE						
	<p>Total : 1920</p>					

237

238



9

239 **Table 3.** Representation of the mass spectrometry data characterizing the oxidation of α -pinene and
 240 limonene (ionization source: HESI positive and negative modes, JSR experiments).

Source and mode	α -Pinene			Limonene		
	HESI ⁺		HESI ⁻	HESI ⁺		HESI ⁻
Number of compounds	594		603	1017		1864
Distribution	specific to positive mode 282	common 312	specific to negative mode 381	specific to positive mode 353	common 482	specific to negative mode 1342
Venn Graph	<p>Mieux ???</p> <p>Total : 975</p>			<p>Total : 2399</p>		
VK vs DBE						
	<p>Total : 2482</p>					

241

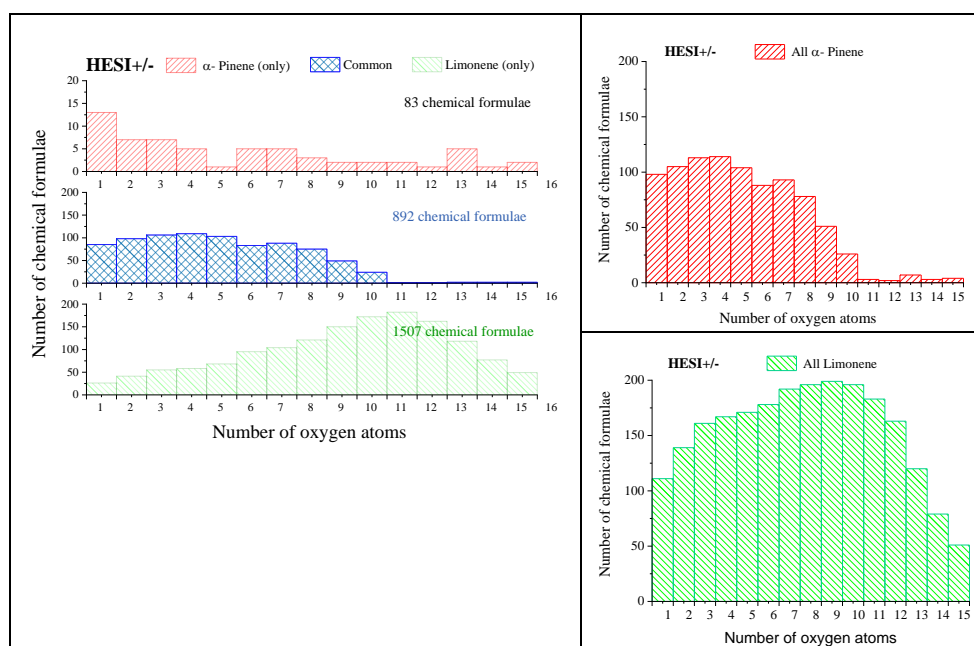
242 *4.2 Autoxidation products detected in a JSR*

243 In order to compare the oxidation of α -pinene and limonene, we compiled the positive and negative ionization data
 244 obtained with APCI (Table 2) and HESI (Table 3) ionization sources to obtain a more exhaustive database. For
 245 the APCI and HESI sources, we distinguished three datasets, two of which are specific to the oxidation of α -pinene



10

246 and limonene and one which is common to both isomers. In the following, the name "only" will be used to describe
247 the molecules specific to the oxidation of one of the terpene isomers. This common dataset represents more than
248 90% of the chemical formulae identified in α -pinene oxidation samples, detected with both APCI and HESI. For
249 limonene, where the number of identified chemical formulae is greater, this common dataset ranges between 68%
250 in APCI and 37% in HESI. In these two cases, the relatively low residence time (2 seconds) and the diversity of
251 the chemical formulae obtained show that the oxidation of these two terpene isomers leads to the opening of the
252 ring, a phenomenon also observed in atmospheric chemistry (Berndt et al., 2016; Zhao et al., 2018; Iyer et al., 2021).
253 Concerning the products' molecular formulae common to both isomers, figure 1 shows that they are limited to 10
254 oxygen atoms. This limit is linked to α -pinene whose oxidation beyond 10 oxygen atoms remains weak (less than
255 2% of the totality of the identified molecules for this isomer). The autoxidation will allow keeping this similarity
256 in the different steps of the oxidation by simple addition of two atoms of oxygen. In the case of limonene, the
257 presence of an exocyclic double bond will increase, in a similar way to atmospheric chemistry (Kundu et al., 2012),
258 the possibilities of oxidation and accretion. It remains however impossible, considering the size of the whole and
259 the diversity of the isomers, to formalize all the reaction mechanisms. Nevertheless, the formation of oxidized
260 species can be described with the help of graphical tools. The dispersion of the number of oxygen atoms per
261 molecule shows for example that limonene oxidizes more than α -pinene (Tables 2 and 3). In the case of limonene,
262 with a HESI source, an oxygen number of up to 15 is measured, with maximum counts recorded for 10 O-atoms
263 (Fig. 1), whereas it remains mostly less than or equal to 10 for α -pinene (Fig. 1). Moreover, this graph shows, for
264 the products specific of limonene oxidation, a distribution centered on 11 oxygen atoms with carbon skeletons
265 probably resulting from accretion.

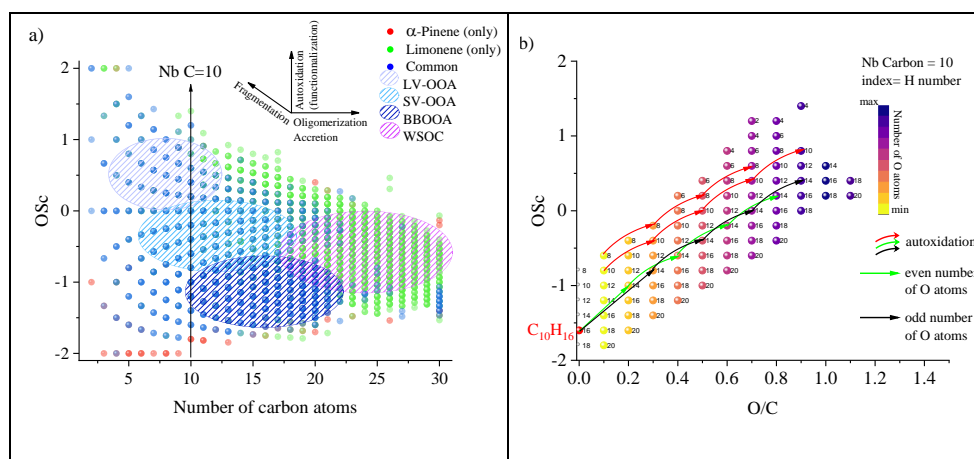


266
267 **Figure 1:** Distribution of α -pinene and limonene autoxidation products as a function of their oxygen content
268 (ionization source: HESI, combined positive and negative modes data).



11

269 To verify this accretion hypothesis, we can plot the OSc as a function of the number of carbon atoms or the O/C
270 ratio at fixed number of C-atoms (Fig. 2). One can visualize the evolution of the molecular oxidation for each
271 carbon skeleton and the formation of oligomers. Species that are unique to one of the isomers, or common to both
272 are differentiated using different colors. In addition to the autoxidation represented by the vertical axes for a given
273 number of carbon atoms (Fig. 2a), we observe mechanisms of fragmentation, accretion and oligomerization
274 between the carbon skeleton. These reaction mechanisms contribute to forming families according to the rate of
275 oxidation and the size of their carbon skeleton. The increase in the number of oxygen atoms, but also of carbon
276 atoms will decrease products volatility. We distinguish four families: low volatile oxygenated organic aerosols
277 (LV-OOA), semi-volatile oxygenated organic aerosols (SV-OOA), biomass burning organic aerosols (BBOA) and
278 water-soluble organic carbons (WSOC) following a classification proposed in the literature (Kroll et al., 2011). If
279 we analyze the two sets of molecules from the APCI and HESI sources, positive and negative ionization modes
280 combined, we find that nearly 73% of the molecules are linked to each other by a single difference of 2 oxygen
281 atoms which reflects an autoxidation mechanism (Fig. 3).

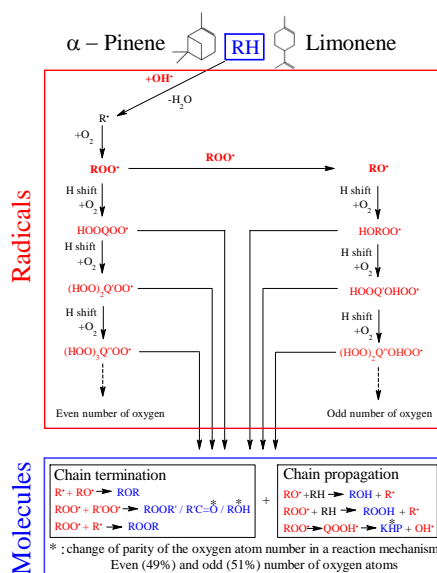


282 **Figure 2:** Overview of the distribution of limonene and α -pinene oxidation products observed in a JSR: (a) OSc
283 versus carbon number in detected chemical formulae from APCI and HESI data. (b) OSc versus O/C atomic ratio
284 for a carbon number of 10; index of the products: number of hydrogen atoms. Arrows indicate autoxidation from
285 a C_6H_{16} isomer, according to the oxygen parity in products.

286 We can measure the amplitude of autoxidation for each carbon skeleton from the OSc vs. O/C space. For the two
287 isomers, for which the initial carbon number (C) is equal to 10, one can observe (Fig. 2b) two autoxidation routes
288 with an even and odd number of oxygen atoms. This parity distinction is initially present for the two main radicals,
289 ROO^{\cdot} and RO^{\cdot} , responsible for autoxidation. However, the termination and propagation reactions will change the
290 oxygen parity to form a new distribution where the parity links between radicals and molecules are lost, making
291 any interpretation of radical oxidation route impossible (Fig. 3). The autoxidation mechanisms indicated by arrows
292 in Figure 2b characterize systematic hydroperoxy chain terminations which do not change oxygen parity. HESI
293 data showed an equivalent distribution of the two oxygen parities in molecular products (odd: 51%; even 49%)
294 therefore confirming a lack of selectivity of the reaction mechanisms with respect to the parity of the radicals.



12



295

296 **Figure 3:** Autoxidation reaction mechanisms in combustion (left) and in the atmosphere (left and right). * indicates
 297 a change in number of oxygen atoms.

298 4.3 Combustion versus atmospheric oxidation

299 We have explored potential chemical pathways related to autoxidation in the previous section. For this purpose,
 300 we have performed experiments under cool flame conditions (590 K). This autoxidation mechanism is also present
 301 in atmospheric chemistry, but it is only recently that it has been found that this mechanism could be one of the
 302 main formation pathways for SOA (Savee et al., 2015). Studies have described this mechanism in the case of
 303 atmospheric chemistry with the identification of radicals and molecular species (Tomaz et al., 2021). However,
 304 previous studies of the propagation of this reaction mechanism are mainly focused on the initial skeletons of the
 305 10-carbon isomers, whereas the other carbon skeletons are also concerned by autoxidation. It is therefore useful to
 306 evaluate the proportion of products of autoxidation among the total species formed.

307 We propose a new approach which consists in assessing a set of molecules mainly resulting from autoxidation
 308 against different sets of experimental studies related to atmospheric chemistry. The objective is to compare the
 309 similarity between these conditions on the basis of autoxidation by considering different experimental parameters
 310 chosen for their diversity. For this purpose, we selected, a HESI ionization source, better adapted to the
 311 electronegativity of the oxidized molecules, as well as to higher m/z. Moreover, we have already shown in this
 312 paper that the HESI (+/-) ionization source is better suited for detecting autoxidation products (detection of 96%
 313 of the total chemical formulae observed in autoxidation).

314 Among published atmospheric chemistry studies of terpenes oxidation, we have selected 15 studies, 4 for α -pinene
 315 and 11 for limonene. The data were acquired using different experimental procedures (methods of oxidation,
 316 techniques of characterization). Table 4 summarizes all the experimental parameters related to the selected studies.

317



13

318 **Table 4.** Experimental settings of 15 oxidation studies of two terpenes under atmospheric conditions and cool
 319 flames.

Reference	Oxidation mode	Sampling	Experimental setup	Concentrations of reactants	Ionization /source	Instrument	Chemical formulae
α-Pinene							
Y. Deng et al. (2021)	Dark ozonolysis seed particles OH scavenger	online	Teflon bag; 0.7m ³	3.3±0.6 ncps ppbv ⁻¹ α -Pinene	ESI	ToF-MS	351
Quéléver et al. (2019)	Ozonolysis	online	Teflon bag 5 m ³	10 & 50 ppb α -Pinene	NO ₃ ⁻ (CI)	CI-API-TOF	68
Meusinger et al. (2017)	Dark Ozonolysis OH scavenger no seed particles	offline	Teflon bag 4.5 m ³	60 ppb α -Pinene	Proton transfer	PTR-MS-ToF	153
Krechmer et al. (2016)	Ozonolysis	offline	PAM Oxidation reactor	Field measurement	ESI (-) and NO ₃ ⁻ (CI)	CI-IMS-ToF	43
This work	Cool-flame autoxidation	offline	jet-stirred reactor	1%, α -Pinene No ozone	APCI(3kV) HESI (3kV)	Orbitrap® Q-Exactive	820 (APCI) 975 (HESI)
Limonene							
Krechmer et al. (2016)	Ozonolysis	offline	PAM Oxidation reactor	not specified	ESI (-) and NO ₃ ⁻ (CI)	CI-IMS-ToF	63
Tomaz et al. (2021)	Ozonolysis	online	flow tube reactor (18 L)	45-227 ppb limonene	NO ₃ ⁻ (CI) - Neg	Orbitrap® Q-Exactive	282
Fang et al. (2017)	OH-initiated photooxidation dark ozonolysis	online	smog chamber	900–1500 ppb limonene	UV; 10 eV	Time-of-Flight (ToF)	17
Witkowski and Gierczak (2017)	Dark ozonolysis	offline	flow reactor	2 ppm, limonene	ESI, 4.5 kV	Triple quadrupole	12
(Jokinen et al., 2015a)	Ozonolysis	online	flow glass tube	1–10000 x10 ⁹ molec.cm ⁻³ , limonene	chemical ionization	Time-of-Flight (ToF)	11
Nørgaard et al. (2013)	Ozone (plasma)	online	direct on the support	850 ppb ozone 15-150 ppb limonene	plasma	Quadrupole time-of-flight (QToF)	29
Bateman et al. (2009)	Dark and UV radiations ozonolysis	offline	Teflon FEP reaction chamber	1 ppm ozone 1 ppm limonene	modified ESI (+/-)	LTQ-Orbitrap Hybrid Mass (ESI)	924
Walser et al. (2008)	Dark ozonolysis	offline	Teflon FEP reaction chamber	1-10 ppm ozone 10 ppm limonene	ESI (+/-); 4.5 kV	LTQ-Orbitrap Hybrid Mass (ESI)	465
Warscheid and Hoffmann (2001)	Ozonolysis	online	Smog chamber	300-500 ppb limonene	APCI; 3kV	Quadrupole ion trap mass	21
Hammes et al., (2019)	Dark ozonolysis	online	flow reactor	15, 40, 150 ppb limonene	²¹⁰ Po α -	HR-ToF-CIMS	20
Kundu et al. (2012)	Dark ozonolysis	offline	Teflon reaction chamber	250 ppb ozone 500 ppb limonene	ESI; 3.7 and 4 kV	LTQ FT Ultra, Thermo Sct (ESI)	1199
This work	Cool-flame autoxidation	offline	jet-stirred reactor	1%, limonene No ozone	APCI(3kV) HESI (3kV)	Orbitrap® Q-Exactive	1863(APCI) 2399(HESI)

320



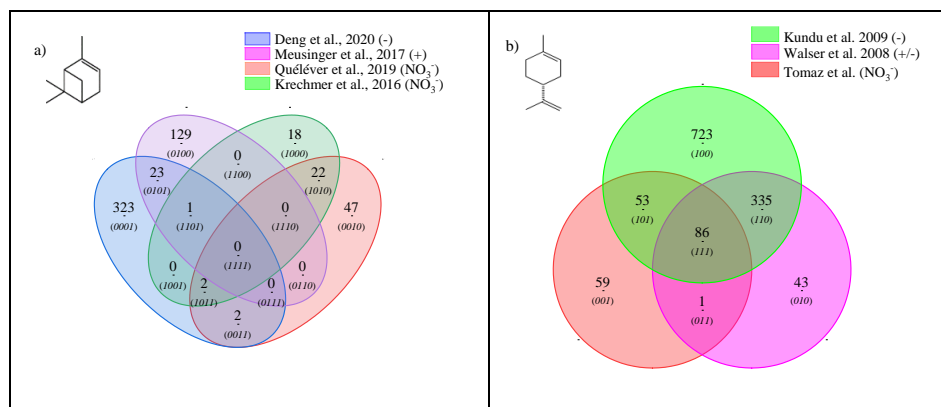
14

321 The data are from the articles or files provided in the supporting information S2. In these studies, oxidation was
322 performed only by ozonolysis with different experimental conditions that gather the main methods described in
323 the literature: ozonolysis, dark ozonolysis, ozonolysis with OH scavenger, ozonolysis with or without seed
324 particles. We considered that the methods of analysis by mass spectrometry did not modify the nature of the
325 chemical species but only their relative importance, because of the type of ionization and the sensitivity of the
326 instruments. The combination of data obtained using (+/-) HESI gives a rather complete picture of the autoxidation
327 products.

328 First, we compared the data from ozonolysis studies of each terpene and identified similarities through the Venn
329 diagram. For studies with two ionization sources, duplicate chemical formulae were removed. We selected the
330 three most representative studies, by the number of the chemical formulae detected. Then, we compared the set of
331 chemical formulae identified after ozonolysis to those produced in low-temperature combustion, the objective
332 being (i) to highlight similarities in terms of products generated by the two oxidation modes and (ii) to identify
333 data resulting from autoxidation.

334 For α -pinene oxidation, the four studies identified 566 chemical formulae, all polarities combined. Only the study
335 by (Meusinger et al., 2017) was performed in positive mode and none of the studies reported data obtained with two
336 ionization modes (+/-). For limonene oxidation, the three studies identified 1862 chemical formulae. Only the
337 studies by (Walser et al., 2008; Bateman et al., 2009) used (+) and (-) ionization modes. In the case of limonene,
338 oxidation for which accretion is more important than for α -pinene, and for which a greater number of chemical
339 formulae were identified, the similarities is more important. These results are presented in Figure 4 where the
340 ionization polarity used in each study is specified.

341



342 **Figure 4:** Venn diagrams for comparing the oxidation results from ozonolysis of (a) α -pinene and (b) limonene
343 (see conditions in Table 1). Each digit of the binary numbers in parentheses identifies the datasets being
344 compared.

345 For α -pinene, no global similarity is observed for the detected chemical formulae. Different hypotheses can be
346 offered to explain this result. Among them, the number of chemical formulae identified per study remains limited
347 (a few dozen to several hundred) and these small datasets are sometimes restricted to specific mass ranges (e.g.



15

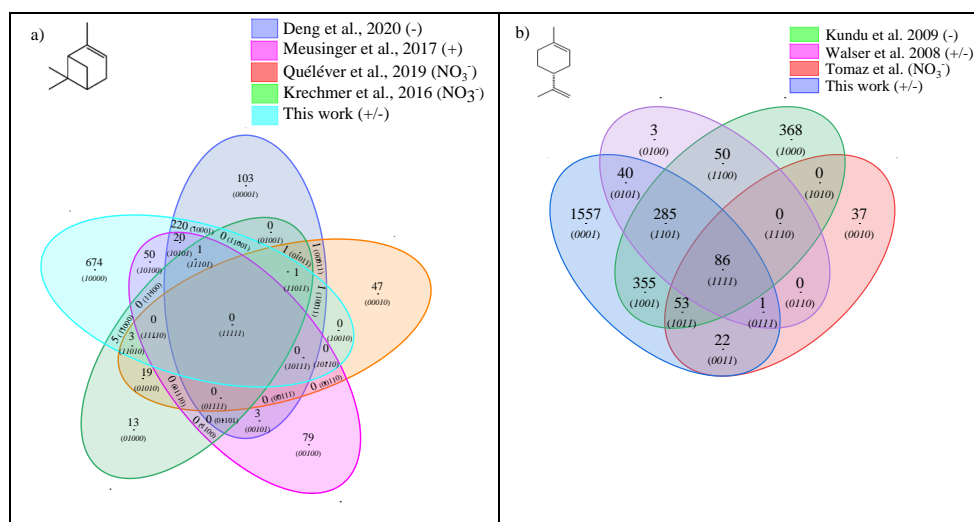
348 (Quéléver et al., 2019): C₁₀ to C₂₀). In the case of studies carried out with an NO₃⁻ source, sensitive to HOMS,
349 produced preferentially by autoxidation, we note that nearly 50% of the chemical formulae (10/22) are linked by
350 a simple difference of 2 oxygen atoms.

351 For limonene, 86 chemical formulae are common to the three studies considered here. In this dataset, nearly 43%
352 of the chemical formulae present a relation similar to that of autoxidation (simple difference of two oxygen atoms)
353 with less than 5% of fragments (Nb C<10). This result seems to indicate that autoxidation dominates.

354 One can then ask if reaction mechanisms common to atmospheric and combustion chemistry can generate, despite
355 radically different experimental conditions, a set of common chemical formulae and if in this common dataset, a
356 common link, characteristic of autoxidation, is observable?

357 To address that question, we compared all the previous results, for each of these terpenes to those obtained under
358 the present combustion study. The comparisons were made using the HESI. One should remember that the
359 oxidation conditions in a JSR were chosen in order to maximize low-temperature autoxidation. Again, we used
360 Venn diagrams to analyze these datasets composed of 1590 chemical formulae in the case of α -pinene and 2857
361 chemical formulae in the case of limonene. The results of these analyses are presented in Figure 5.

362 It turned out that 301 chemical formulae were identified for α -pinene and 735 chemical formulae for limonene to
363 be common to oxidation by ozonolysis and combustion. This represents 31% of the chemical formulae for the
364 ozonolysis of α -pinene and 31% for those of limonene ozonolysis. For α -pinene, the similarities compared to
365 combustion are specific to each study: (Deng et al., 2021) 69% (Meusinger et al., 2017) 46% (Quéléver et al.,
366 2019) 7% (Krechmer et al., 2016) 23%. Chemical formulae common to all studies were not identified. This lack of
367 similarity may be due to a partial characterization of the chemical formulae, a weaker oxidation of α -pinene with
368 an ionization mode less favorable to low molecular weights.

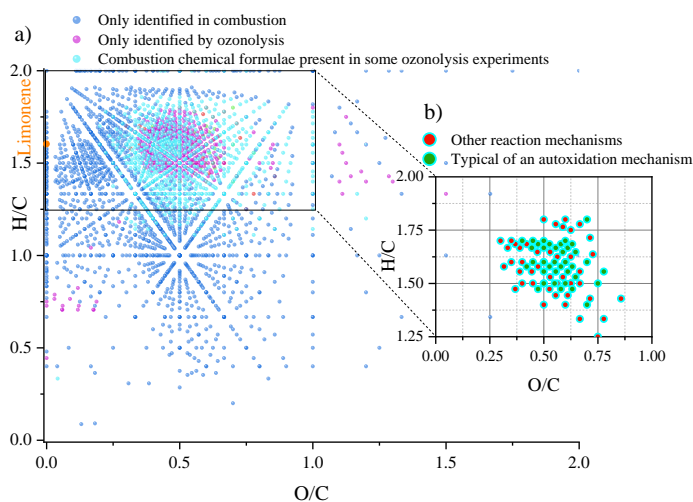


369 **Figure 5:** Venn diagrams comparing the oxidation results from ozonolysis and combustion of (a) α -pinene and
370 (b) limonene (see conditions in Table 1).



16

371 For limonene, the similarities with combustion are more important and less spread out. They represent for the
372 different studies: (Kundu et al., 2012) 65% (Walser et al., 2008) 88% (Tomaz et al., 2021) 81%. Moreover, there
373 is a common dataset of 86 chemical formulae which can derive from autoxidation mechanisms. It is necessary to
374 specify again that different reaction mechanisms can cause the observed similarities. However, the preponderance
375 of autoxidation in so-called cold flame combustion is obvious, and in atmospheric chemistry, this reaction
376 mechanism remains competitive or dominates (Crouse et al., 2013; Jokinen et al., 2014b). If we search for an
377 autoxidation link between these 86 chemical formulae, we observe that 43% of these chemical formulae meet this
378 condition: difference of two oxygen atoms, at constant number of carbon and hydrogen atoms. More precisely,
379 these molecules are centered in a van Krevelen diagram on the ratios $O/C=0.6$ and $H/C=1.6$, in the range $0.25 <$
380 $O/C < 0.8$ and $1.25 < H/C < 1.85$. All oxidized molecules associated with this dataset are presented in Figure 6.
381 The dispersion of the chemical formulae, far from being random, remains consistent with an autoxidation
382 mechanism where the number of carbon atoms is constant.



383

384 **Figure 6:** Van Krevelen diagram showing specific and common chemical formulae detected after to oxidation of
385 limonene by ozonolysis and combustion.

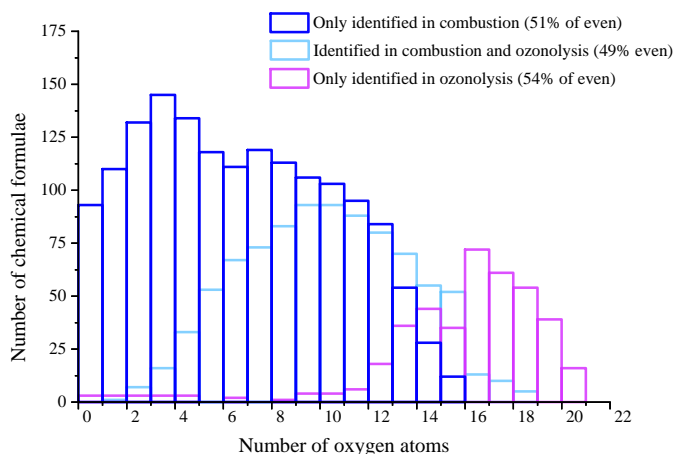
386 A 3-D representation of all limonene oxidation data is given in Fig. S1 (Supplement) where DBE is used as third
387 dimension. From that figure, one can note that products with higher DBE are preferably formed under JSR
388 conditions, i.e. at elevated temperature. The corresponding chemical formulae could correspond to carbonyls and
389 / or cyclic ethers ($^{\bullet}QOOH \rightarrow$ carbonyl + alkene + OH and / or cyclic ether + OH).

390



17

391 Specificities and similarities of these two oxidation modes were further investigated by plotting the distribution of
392 the number of oxygen atoms in detected chemical formulae (Fig. 7). Indeed, the distribution of the number of
393 oxygen atoms allows, in addition to the Van Krevelen diagram, to provide some additional details on these two
394 modes of oxidation. It is in ozonolysis that we observe the chemical formulae having the largest number of oxygen
395 atoms. There, oxidation proceeds over a long reaction time where the phenomenon of aging appears by promoting
396 accretion or oligomerization. One should keep in mind that a short residence time (2 s) was used in JSR
397 experiments. A short residence time should limit accretion which is favored under simulated atmospheric oxidation
398 experiments performed over long reaction times. In combustion, the number of oxygen atoms remains limited to
399 18, with a lower number of detected chemical formulae compared to the case of ozonolysis. However, it is in
400 combustion that we observe the highest O/C ratios, indicating the formation of the most oxidized products. This
401 difference, however, does not affect the similarities between the chemical formulae detected in the two modes of
402 oxidation. Finally, the analysis of the parities in oxygen atoms, very similar to the three datasets, confirms that the
403 reaction mechanisms presented in Figure 3 do not allow a simple link to be established between the parity of
404 radicals and that of molecular products.



405
406 **Figure 7:** Oxygen number distribution for all the molecules identified for the oxidation of limonene: only in
407 combustion, only in ozonolysis and common to both processes. For each of these distributions, the parity in
408 oxygen number is specified

409 5 Conclusion

410 We have analyzed and compared, thanks to different mathematical and visualization tools, the oxidation of α -
411 pinene and limonene under simulated tropospheric and low-temperature oxidation conditions. We have restricted
412 the field of this study to organic compounds ($C_nH_yO_z$) in order to study specifically autoxidation. This work is in
413 the continuity of recently published studies which established the importance of autoxidation under tropospheric
414 oxidation and low-temperature combustion conditions. Faced with the analytical limits of the chemical speciation
415 of thousands of molecules, and in order to complete the work carried out on the reaction mechanisms of the first
416 steps of oxidation, we have developed a global approach based on the study of families of chemical compounds
417 present in these large sets (van Krevelen diagram, oxygen number distribution, oxidation state of carbon -OSc,



18

418 chemical relationship between molecules). We selected existing databases on ozonolysis with a purposive diversity
419 of experimental conditions and compared these data to those obtained in low-temperature combustion conditions
420 where autoxidation is important (cool flame combustion at 590 K). We showed that a significant portion of the
421 chemical formulae were common to both atmospheric and combustion products. Surprisingly, the numerous
422 oxidation mechanisms and the isomerization of chemical species proceeding under these two conditions did not
423 lead to diverging data, but, on the contrary, to similarities. More than 35% of the chemical formulae detected in
424 combustion chemistry experiments using a JSR have been detected in the studies carried out under atmospheric
425 conditions. Finally, we have outlined the existence of a substantial common dataset of autoxidation products. This
426 result tends to show that autoxidation is indeed inducing similarity between atmospheric and combustion products.

427 Acknowledgements

428 The authors gratefully acknowledge funding from the Labex Caprysses (ANR-11-LABX-0006-01), the Labex
429 Voltaire (ANR-10-LABX-100-01), CPER, and EFRD (PROMESTOCK and APPROPOR-e projects). We also
430 thank Matthieu RIVA for sharing his experimental data on limonene oxidation.

431

432 References

- 433 Barsanti, K. C., Kroll, J. H., and Thornton, J. A.: Formation of Low-Volatility Organic Compounds in the
434 Atmosphere: Recent Advancements and Insights, *J Phys Chem Lett*, 8, 1503-1511, 10.1021/acs.jpcllett.6b02969,
435 2017.
- 436 Bateman, A. P., Nizkorodov, S. A., Laskin, J., and Laskin, A.: Time-resolved molecular characterization of
437 limonene/ozone aerosol using high-resolution electrospray ionization mass spectrometry, *Physical Chemistry
438 Chemical Physics*, 11, 7931-7942, 10.1039/B905288G, 2009.
- 439 Belhadj, N., Benoit, R., Dagaut, P., Lailliau, M., Serinyel, Z., Dayma, G., Khaled, F., Moreau, B., and Foucher,
440 F.: Oxidation of di-n-butyl ether: Experimental characterization of low-temperature products in JSR and RCM,
441 *Combustion and Flame*, 222, 133-144, <https://doi.org/10.1016/j.combustflame.2020.08.037>, 2020.
- 442 Belhadj, N., Lailliau, M., Benoit, R., and Dagaut, P.: Experimental and kinetic modeling study of n-hexane
443 oxidation. Detection of complex low-temperature products using high-resolution mass spectrometry,
444 *Combustion and Flame*, 233, 111581, <https://doi.org/10.1016/j.combustflame.2021.111581>, 2021.
- 445 Benoit, R., Belhadj, N., Lailliau, M., and Dagaut, P.: On the similarities and differences between the products of
446 oxidation of hydrocarbons under simulated atmospheric conditions and cool flames, *Atmos. Chem. Phys.*, 21,
447 7845-7862, 10.5194/acp-21-7845-2021, 2021.
- 448 Berndt, T., Richters, S., Kaethner, R., Voigtländer, J., Stratmann, F., Sipilä, M., Kulmala, M., and Herrmann, H.:
449 Gas-Phase Ozonolysis of Cycloalkenes: Formation of Highly Oxidized RO₂ Radicals and Their Reactions with
450 NO, NO₂, SO₂, and Other RO₂ Radicals, *The Journal of Physical Chemistry A*, 119, 10336-10348,
451 10.1021/acs.jpca.5b07295, 2015.
- 452 Berndt, T., Richters, S., Jokinen, T., Hyttinen, N., Kurtén, T., Otkjær, R. V., Kjaergaard, H. G., Stratmann, F.,
453 Herrmann, H., Sipilä, M., Kulmala, M., and Ehn, M.: Hydroxyl radical-induced formation of highly oxidized
454 organic compounds, *Nature Communications*, 7, 13677, 10.1038/ncomms13677, 2016.
- 455 Bianchi, F., Kurtén, T., Riva, M., Mohr, C., Rissanen, M. P., Roldin, P., Berndt, T., Crouse, J. D., Wennberg, P.
456 O., Mentel, T. F., Wildt, J., Junninen, H., Jokinen, T., Kulmala, M., Worsnop, D. R., Thornton, J. A., Donahue,
457 N., Kjaergaard, H. G., and Ehn, M.: Highly Oxygenated Organic Molecules (HOM) from Gas-Phase
458 Autoxidation Involving Peroxy Radicals: A Key Contributor to Atmospheric Aerosol, *Chemical Reviews*, 119,
459 3472-3509, 10.1021/acs.chemrev.8b00395, 2019.
- 460 Crouse, J. D., Nielsen, L. B., Jørgensen, S., Kjaergaard, H. G., and Wennberg, P. O.: Autoxidation of organic
461 compounds in the atmosphere, *J. Phys. Chem. Lett.*, 4, 3513, 2013.
- 462 Dagaut, P., Cathonnet, M., Rouan, J. P., Foulatier, R., Quilgars, A., Boettner, J. C., Gaillard, F., and James, H.:
463 A jet-stirred reactor for kinetic studies of homogeneous gas-phase reactions at pressures up to ten atmospheres
464 (≈ 1 MPa), *Journal of Physics E: Scientific Instruments*, 19, 207-209, 10.1088/0022-3735/19/3/009, 1986.
- 465 Dagaut, P., Cathonnet, M., Boettner, J. C., and Gaillard, F.: Kinetic Modeling of Propane Oxidation, *Combustion
466 Science and Technology*, 56, 23-63, 10.1080/00102208708947080, 1987.
- 467 Dagaut, P., Cathonnet, M., Boettner, J. C., and Gaillard, F.: Kinetic modeling of ethylene oxidation, *Combustion
468 and Flame*, 71, 295-312, [https://doi.org/10.1016/0010-2180\(88\)90065-X](https://doi.org/10.1016/0010-2180(88)90065-X), 1988.



- 469 Deng, Y., Inomata, S., Sato, K., Ramasamy, S., Morino, Y., Enami, S., and Tanimoto, H.: Temperature and
470 acidity dependence of secondary organic aerosol formation from α -pinene ozonolysis with a compact chamber
471 system, *Atmos. Chem. Phys.*, 21, 5983-6003, 10.5194/acp-21-5983-2021, 2021.
- 472 Fang, W., Gong, L., and Sheng, L.: Online analysis of secondary organic aerosols from OH-initiated
473 photooxidation and ozonolysis of α -pinene, β -pinene, Δ^3 -carene and d-limonene by thermal desorption-
474 photoionisation aerosol mass spectrometry, *Environmental Chemistry*, 14, 75-90,
475 <https://doi.org/10.1071/EN16128>, 2017.
- 476 Hammes, J., Lutz, A., Mentel, T., Faxon, C., and Hallquist, M.: Carboxylic acids from limonene oxidation by
477 ozone and hydroxyl radicals: insights into mechanisms derived using a FIGAERO-CIMS, *Atmos. Chem. Phys.*,
478 19, 13037-13052, 10.5194/acp-19-13037-2019, 2019.
- 479 Hecht, E. S., Scigelova, M., Eliuk, S., and Makarov, A.: Fundamentals and Advances of Orbitrap Mass
480 Spectrometry, in: *Encyclopedia of Analytical Chemistry*, 1-40, 2019.
- 481 Huang, W., Saathoff, H., Pajunoja, A., Shen, X., Naumann, K. H., Wagner, R., Virtanen, A., Leisner, T., and
482 Mohr, C.: α -Pinene secondary organic aerosol at low temperature: chemical composition and implications for
483 particle viscosity, *Atmos. Chem. Phys.*, 18, 2883-2898, 10.5194/acp-18-2883-2018, 2018.
- 484 Iyer, S., Rissanen, M. P., Valiev, R., Barua, S., Krechmer, J. E., Thornton, J., Ehn, M., and Kurtén, T.: Molecular
485 mechanism for rapid autoxidation in α -pinene ozonolysis, *Nature Communications*, 12, 878, 10.1038/s41467-
486 021-21172-w, 2021.
- 487 Jokinen, T., Sipilä, M., Richters, S., Kerminen, V.-M., Paasonen, P., Stratmann, F., Worsnop, D., Kulmala, M.,
488 Ehn, M., Herrmann, H., and Berndt, T.: Rapid Autoxidation Forms Highly Oxidized RO₂ Radicals in the
489 Atmosphere, *Angewandte Chemie International Edition*, 53, 14596-14600,
490 <https://doi.org/10.1002/anie.201408566>, 2014a.
- 491 Jokinen, T., Sipilä, M., Richters, S., Kerminen, V. M., Paasonen, P., Stratmann, F., Worsnop, D., Kulmala, M.,
492 Ehn, M., and Herrmann, H.: Rapid autoxidation forms highly oxidized RO₂ radicals in the atmosphere, *Angew.*
493 *Chem., Int. Ed.*, 53, 14596, 2014b.
- 494 Jokinen, T., Berndt, T., Makkonen, R., Kerminen, V.-M., Junninen, H., Paasonen, P., Stratmann, F., Herrmann,
495 H., Guenther, A. B., Worsnop, D. R., Kulmala, M., Ehn, M., and Sipilä, M.: Production of extremely low
496 volatile organic compounds from biogenic emissions: Measured yields and atmospheric implications,
497 *Proceedings of the National Academy of Sciences*, 112, 7123-7128, 10.1073/pnas.1423977112, 2015a.
- 498 Jokinen, T., Berndt, T., Makkonen, R., Kerminen, V.-M., Junninen, H., Paasonen, P., Stratmann, F., Herrmann,
499 H., Guenther, A. B., Worsnop, D. R., Kulmala, M., Ehn, M., and Sipilä, M.: Production of extremely low
500 volatile organic compounds from biogenic emissions: Measured yields and atmospheric implications,
501 *Proceedings of the National Academy of Sciences*, 112, 7123, 10.1073/pnas.1423977112, 2015b.
- 502 Kenseth, C. M., Huang, Y., Zhao, R., Dalleska, N. F., Hethcox, J. C., Stoltz, B. M., and Seinfeld, J. H.:
503 Synergistic O₃ + OH oxidation pathway to extremely low-volatility dimers revealed in β -pinene secondary
504 organic aerosol, *Proceedings of the National Academy of Sciences*, 201804671, 10.1073/pnas.1804671115,
505 2018.
- 506 Kourtchev, I., Doussin, J. F., Giorio, C., Mahon, B., Wilson, E. M., Maurin, N., Pangui, E., Venables, D. S.,
507 Wenger, J. C., and Kalberer, M.: Molecular Composition of Fresh and Aged Secondary Organic Aerosol from a
508 Mixture of Biogenic Volatile Compounds: A High-Resolution Mass Spectrometry Study, *Atmos. Chem. Phys.*,
509 15, 5683, 2015.
- 510 Krechmer, J. E., Groessl, M., Zhang, X., Junninen, H., Massoli, P., Lambe, A. T., Kimmel, J. R., Cubison, M. J.,
511 Graf, S., Lin, Y. H., Budisulistiorini, S. H., Zhang, H., Surratt, J. D., Knochenmuss, R., Jayne, J. T., Worsnop, D.
512 R., Jimenez, J. L., and Canagaratna, M. R.: Ion mobility spectrometry-mass spectrometry (IMS-MS) for on- and
513 offline analysis of atmospheric gas and aerosol species, *Atmos. Meas. Tech.*, 9, 3245-3262, 10.5194/amt-9-3245-
514 2016, 2016.
- 515 Kristensen, K., Watne, Å. K., Hammes, J., Lutz, A., Petäjä, T., Hallquist, M., Bilde, M., and Glasius, M.: High-
516 Molecular Weight Dimer Esters Are Major Products in Aerosols from α -Pinene Ozonolysis and the Boreal
517 Forest, *Environmental Science & Technology Letters*, 3, 280-285, 10.1021/acs.estlett.6b00152, 2016.
- 518 Kroll, J. H., Donahue, N. M., Jimenez, J. L., Kessler, S. H., Canagaratna, M. R., Wilson, K. R., Altieri, K. E.,
519 Mazzoleni, L. R., Wozniak, A. S., Bluhm, H., Mysak, E. R., Smith, J. D., Kolb, C. E., and Worsnop, D. R.:
520 Carbon oxidation state as a metric for describing the chemistry of atmospheric organic aerosol, *Nature*
521 *Chemistry*, 3, 133-139, 10.1038/nchem.948, 2011.
- 522 Kundu, S., Fisseha, R., Putman, A. L., Rahn, T. A., and Mazzoleni, L. R.: High molecular weight SOA
523 formation during limonene ozonolysis: insights from ultrahigh-resolution FT-ICR mass spectrometry
524 characterization, *Atmos. Chem. Phys.*, 12, 5523-5536, 10.5194/acp-12-5523-2012, 2012.
- 525 Kurtén, T., Rissanen, M. P., Mackeprang, K., Thornton, J. A., Hyttinen, N., Jørgensen, S., Ehn, M., and
526 Kjaergaard, H. G.: Computational Study of Hydrogen Shifts and Ring-Opening Mechanisms in α -Pinene
527 Ozonolysis Products, *The Journal of Physical Chemistry A*, 119, 11366-11375, 10.1021/acs.jpca.5b08948, 2015.



20

- 528 Melendez-Perez, J. J., Martínez-Mejía, M. J., and Eberlin, M. N.: A reformulated aromaticity index equation
529 under consideration for non-aromatic and non-condensed aromatic cyclic carbonyl compounds, *Organic*
530 *Geochemistry*, 95, 29-33, <https://doi.org/10.1016/j.orggeochem.2016.02.002>, 2016.
- 531 Meusinger, C., Dusek, U., King, S. M., Holzinger, R., Rosenørn, T., Sperlich, P., Julien, M., Remaud, G. S.,
532 Bilde, M., Röckmann, T., and Johnson, M. S.: Chemical and isotopic composition of secondary organic aerosol
533 generated by α -pinene ozonolysis, *Atmos. Chem. Phys.*, 17, 6373-6391, 10.5194/acp-17-6373-2017, 2017.
- 534 Nørgaard, A. W., Vibenholt, A., Benassi, M., Clausen, P. A., and Wolkoff, P.: Study of Ozone-Initiated
535 Limonene Reaction Products by Low Temperature Plasma Ionization Mass Spectrometry, *Journal of The*
536 *American Society for Mass Spectrometry*, 24, 1090-1096, 10.1007/s13361-013-0648-3, 2013.
- 537 Nozière, B., Kalberer, M., Claeys, M., Allan, J., D'Anna, B., Decesari, S., Finessi, E., Glasius, M., Grgić, I.,
538 Hamilton, J. F., Hoffmann, T., Iinuma, Y., Jaoui, M., Kahnt, A., Kampf, C. J., Kourtchev, I., Maenhaut, W.,
539 Marsden, N., Saarikoski, S., Schnelle-Kreis, J., Surratt, J. D., Szidat, S., Szmigielski, R., and Wisthaler, A.: The
540 Molecular Identification of Organic Compounds in the Atmosphere: State of the Art and Challenges, *Chemical*
541 *Reviews*, 115, 3919-3983, 10.1021/cr5003485, 2015.
- 542 Otkjær, R. V., Jakobsen, H. H., Tram, C. M., and Kjaergaard, H. G.: Calculated Hydrogen Shift Rate Constants
543 in Substituted Alkyl Peroxy Radicals, *The Journal of Physical Chemistry A*, 122, 8665-8673,
544 10.1021/acs.jpca.8b06223, 2018.
- 545 Pospisilova, V., Lopez-Hilfiker, F. D., Bell, D. M., El Haddad, I., Mohr, C., Huang, W., Heikkinen, L., Xiao, M.,
546 Dommen, J., Prevot, A. S. H., Baltensperger, U., and Slowik, J. G.: On the fate of oxygenated organic molecules
547 in atmospheric aerosol particles, *Science Advances*, 6, eaax8922, 10.1126/sciadv.aax8922, 2020.
- 548 Quéléver, L. L. J., Kristensen, K., Normann Jensen, L., Rosati, B., Teiwes, R., Daellenbach, K. R., Peräkylä, O.,
549 Roldin, P., Bossi, R., Pedersen, H. B., Glasius, M., Bilde, M., and Ehn, M.: Effect of temperature on the
550 formation of highly oxygenated organic molecules (HOMs) from alpha-pinene ozonolysis, *Atmos. Chem. Phys.*,
551 19, 7609-7625, 10.5194/acp-19-7609-2019, 2019.
- 552 Savee, J. D., Papajak, E., Rotavera, B., Huang, H., Eskola, A. J., Welz, O., Sheps, L., Taatjes, C. A., Zádor, J.,
553 and Osborn, D. L.: Carbon radicals. Direct observation and kinetics of a hydroperoxyalkyl radical (QOOH),
554 *Science*, 347, 643-646, 10.1126/science.aaa1495, 2015.
- 555 Shrivastava, M., Cappa, C. D., Fan, J. W., Goldstein, A. H., Guenther, A. B., Jimenez, J. L., Kuang, C., Laskin,
556 A., Martin, S. T., Ng, N. L., Petaja, T., Pierce, J. R., Rasch, P. J., Roldin, P., Seinfeld, J. H., Shilling, J., Smith, J.
557 N., Thornton, J. A., Volkamer, R., Wang, J., Worsnop, D. R., Zaveri, R. A., Zelenyuk, A., and Zhang, Q.: Recent
558 advances in understanding secondary organic aerosol: Implications for global climate forcing, *Rev. Geophys.*,
559 55, 509, 2017.
- 560 Tomaz, S., Wang, D., Zabalegui, N., Li, D., Lamkaddam, H., Bachmeier, F., Vogel, A., Monge, M. E., Perrier,
561 S., Baltensperger, U., George, C., Rissanen, M., Ehn, M., El Haddad, I., and Riva, M.: Structures and reactivity
562 of peroxy radicals and dimeric products revealed by online tandem mass spectrometry, *Nature Communications*,
563 12, 300, 10.1038/s41467-020-20532-2, 2021.
- 564 Tröstl, J., Chuang, W. K., Gordon, H., Heinritzi, M., Yan, C., Molteni, U., Ahlm, L., Frege, C., Bianchi, F.,
565 Wagner, R., Simon, M., Lehtipalo, K., Williamson, C., Craven, J. S., Duplissy, J., Adamov, A., Almeida, J.,
566 Bernhammer, A.-K., Breitenlechner, M., Brilke, S., Dias, A., Ehrhart, S., Flagan, R. C., Franchin, A., Fuchs, C.,
567 Guida, R., Gysel, M., Hansel, A., Hoyle, C. R., Jokinen, T., Junninen, H., Kangasluoma, J., Keskinen, H., Kim,
568 J., Krapf, M., Kürten, A., Laaksonen, A., Lawler, M., Leiminger, M., Mathot, S., Möhler, O., Nieminen, T.,
569 Onnela, A., Petäjä, T., Piel, F. M., Miettinen, P., Rissanen, M. P., Rondo, L., Sarnela, N., Schobesberger, S.,
570 Sengupta, K., Sipilä, M., Smith, J. N., Steiner, G., Tomè, A., Virtanen, A., Wagner, A. C., Weingartner, E.,
571 Wimmer, D., Winkler, P. M., Ye, P., Carslaw, K. S., Curtius, J., Dommen, J., Kirkby, J., Kulmala, M., Riipinen,
572 I., Worsnop, D. R., Donahue, N. M., and Baltensperger, U.: The role of low-volatility organic compounds in
573 initial particle growth in the atmosphere, *Nature*, 533, 527-531, 10.1038/nature18271, 2016.
- 574 Van Krevelen, D. W.: Graphical-statistical method for the study of structure and reaction processes of coal, *Fuel*,
575 29, 269-284, 1950.
- 576 Vereecken, L., Müller, J. F., and Peeters, J.: Low-volatility poly-oxygenates in the OH-initiated atmospheric
577 oxidation of α -pinene: impact of non-traditional peroxy radical chemistry, *Physical Chemistry Chemical*
578 *Physics*, 9, 5241-5248, 10.1039/B708023A, 2007.
- 579 Walser, M. L., Desyaterik, Y., Laskin, J., Laskin, A., and Nizkorodov, S. A.: High-resolution mass spectrometric
580 analysis of secondary organic aerosol produced by ozonation of limonene, *Physical Chemistry Chemical*
581 *Physics*, 10, 1009-1022, 10.1039/B712620D, 2008.
- 582 Wang, Z., Ehn, M., Rissanen, M. P., Garmash, O., Quéléver, L., Xing, L., Monge Palacios, M., Rantala, P.,
583 Donahue, N. M., Berndt, T., and Sarathy, M.: - Efficient alkane oxidation under combustion engine and
584 atmospheric conditions, - Springer Science and Business Media LLC, 2021.
- 585 Warscheid, B., and Hoffmann, T.: Structural elucidation of monoterpene oxidation products by ion trap
586 fragmentation using on-line atmospheric pressure chemical ionisation mass spectrometry in the negative ion
587 mode, *Rapid Communications in Mass Spectrometry*, 15, 2259-2272, 10.1002/rcm.504, 2001.



21

- 588 Witkowski, B., and Gierczak, T.: Characterization of the limonene oxidation products with liquid
589 chromatography coupled to the tandem mass spectrometry, *Atmospheric Environment*, 154, 297-307,
590 <https://doi.org/10.1016/j.atmosenv.2017.02.005>, 2017.
- 591 Xie, Q., Su, S., Chen, S., Xu, Y., Cao, D., Chen, J., Ren, L., Yue, S., Zhao, W., Sun, Y., Wang, Z., Tong, H., Su,
592 H., Cheng, Y., Kawamura, K., Jiang, G., Liu, C. Q., and Fu, P.: Molecular characterization of firework-related
593 urban aerosols using Fourier transform ion cyclotron resonance mass spectrometry, *Atmos. Chem. Phys.*, 20,
594 6803-6820, 10.5194/acp-20-6803-2020, 2020.
- 595 Zhao, Y., Thornton, J. A., and Pye, H. O. T.: Quantitative constraints on autoxidation and dimer formation from
596 direct probing of monoterpene-derived peroxy radical chemistry, *Proc Natl Acad Sci U S A*, 115, 12142-12147,
597 10.1073/pnas.1812147115, 2018.
- 598